BNL-203550-2018-TECH
C-A/AP/602

A state of the art current-septum dipole magnet

N. Tsoupas

April 2018

Collider Accelerator Department
Brookhaven National Laboratory

U.S. Department of Energy
USDOE Office of Science (SC), Nuclear Physics (NP) (SC-26)

DISCLAIMER

A STATE OF THE ART CURRENT-SEPTUM DIPOLE MAGNET

N. Tsoupas, K. Brown, F. Méot, C. Pearson, P. Pile, V. Ptitsyn, A. Rusek

ABSTRACT

The acceleration process of charged particle beams often requires the use of few acceleration stages to provide the beam with the desired energy. The extraction of the beam from one acceleration stage and the injection to the next, both require a special type of magnet which comes under the name septum magnet. Such a magnet generates a strong field in one region of space and a very low field in another region with the two regions separated by a very thin material (septum). The septum thickness of such a magnet should be as thin as possible to reduce the strength of other devices, like kickers, which are involved in the extraction or injection processes. A thin septum is also advantageous during the slow beam extraction process to reduce the beam losses at the septum. One of the methods which in theory can generate very large differences in field strength in adjacent field regions separated by a thin septum, is the use of two thin parallel current sheets of infinite dimensions. In practice we use other devices that can approximate such an abrupt change of the magnetic field within the septum thickness. In this paper we describe such a device, the DC current septum, we present results from the study of its electromagnetic properties, and we provide a method to minimize the magnetic field in the region which requires a very small magnetic field. We also provide some experimental measurements of the magnetic field generated by the "D6" current septum magnet which is installed in the experimental beam line of the NASA's Space Radiation Laboratory (NSRL) facility [1,2] at Brookhaven National Laboratory and its function is to extract ion beams from the AGS-Booster into the NSRL beam line for material and biological studies.

INTRODUCTION

In an accelerator complex an ion beam undergoes a few acceleration stages during which the beam is extracted from one accelerator and injected into another. This extraction/injection process requires devices which can maintain high magnetic field in one region of space and a very low magnetic field in a region adjacent to the high field one, with the two regions separated by a thin septum. The thinner the septum the lower the strength of the kicker magnet which is a device associated with the beam's injection or extraction process. A thin septum is also beneficial during the slow beam extraction process from an accelerator, to reduce the beam losses at the septum. An ideal septum magnet can be made by two parallel infinite current sheets having current densities J of equal magnitude, and opposite directions as shown schematically with the green arrows in Fig. 1.

The parallel current sheets generate a uniform magnetic field within the region of the plates and zero magnetic field in the regions outside the plates. Such a septum magnet as shown in Fig. 1 is not realistic but it can be replaced by two finite parallel current sheets placed within a "C-shape" magnetic material of infinite magnetic permeability as shown in the left picture of Fig. 2. Such a "C-shape" magnet can generate a uniform magnetic field within the gap of the iron and the strength of this uniform field can be easily calculated using Ampere's law or it can be calculated as the field generated within the two infinite current sheets shown in the right side of the picture. The current sheets have equal and opposite current densities (J_- , J_+) and are generated from the images of the current regions which are within the magnet in the left picture.

A cross section of a more realistic current septum is shown in the left picture of Fig. 3 where the current carrying conductors (red rectangles within the C-magnet) are not in conduct with the iron of the magnet and the permeability of the magnetic material is finite.

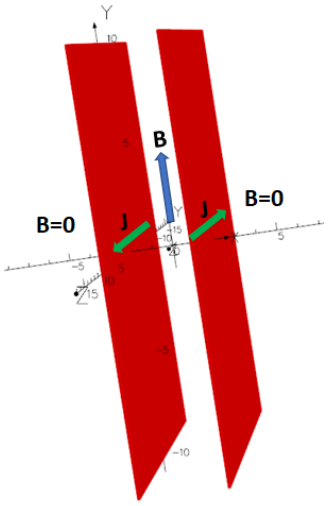

Figure 1: A schematic diagram of two parallel current sheets of infinite size having current densities of equal magnitude and opposite direction (green arrows) generate a uniform magnetic field in the region within the plates and zero magnetic field in the regions outside the plates.

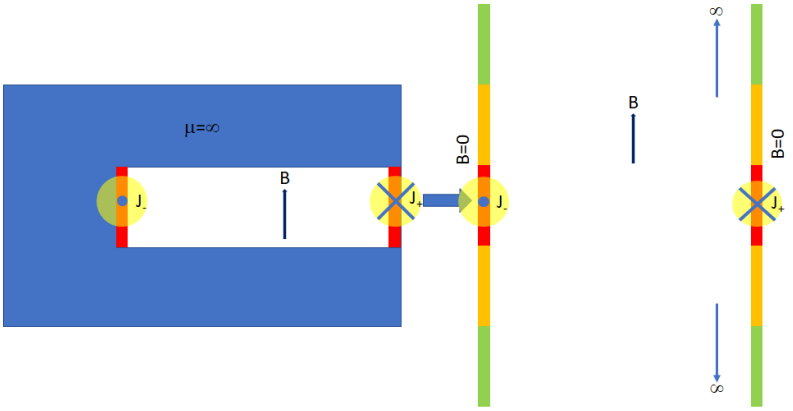

Figure 2: A current septum magnet (left) consists of magnetic material of infinite permeability (area of blue color) with two current sheets (red rectangles within the gap of the iron) with current densities equal in magnitude and opposite direction. The field within the gap of the magnet is uniform and its magnitude is equal to that generated between two infinite current sheets, with equal and opposite current densities, shown in the right picture of this figure.

The field within the gap of the magnet and the field to the outside region of the magnet, can be calculated using the image current method which generates the segmented current carrying conductors shown on the right picture with different colors. As the distance of the conductors increases from the median plane, their current density of each conductor decreases because of the iron's finite value of permeability. The segmented current carrying conductors on the right side of the picture generate a magnetic field within the region of the conductors with acceptable field uniformity and also generate a relatively small magnetic field in the regions outside. Since the permeability of the iron is not linear with the H field and also the computation of a three dimensional field is required for the complete electromagnetic study of the magnet, the OPERA computer code [3] is used to calculate the B field of the septum magnet. The design of the current septum magnet aims to minimizes the magnetic field outside of the main field region, and generate a magnetic field in the main field region with acceptable field uniformity.

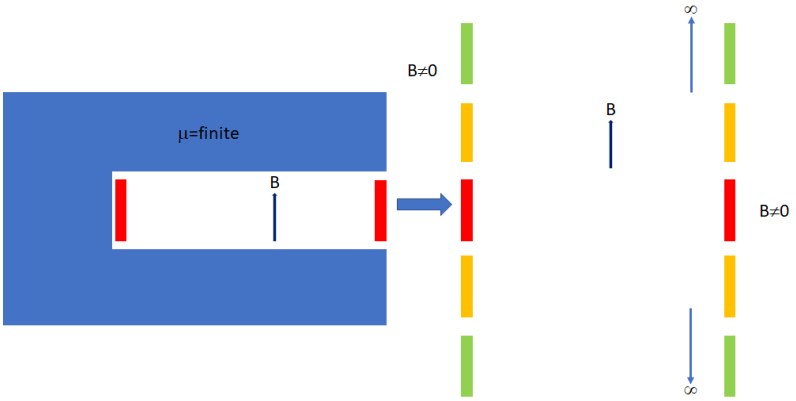

Figure 3: . A realistic current septum magnet (left) which consists of magnetic material with finite permeability (blue color regions) with two current sheets (red rectangles) not touching the magnetic material, and having current densities of opposite direction. The method of image currents makes the current septum magnet (left) equivalent to an infinite number of current carrying conductors which do not touch each other as shown in the right picture of this figure. Moreover, due to the finite permeability of the magnetic material, the segmented conductors carry diminishing current densities with increasing distance of the conductors from the median plane.

ELECTROMAGNETIC DESIGN OF A CURRENT SEPTUM DIPOLE MAGNET

In this section we present results from the electromagnetic design of the current septum dipole magnet (D6) which extracts the ion beams from the AGS-Booster into the beam line of the NSRL facility [1,2] at the Brookhaven National Laboratory. The study of the D6 model magnet has been performed using the 2D and the 3D-TOSCA modules of the OPERA computer code [3] and the next two subsections are devoted in the 2D and 3D-TOSCA study respectively of the magnet. Table 1 lists some specifications of the D6 magnet including the maximum field and rigidity of the deflected particles.

Table 1: Some specifications of the D6 Septum Magnet.

Length [m]	Gap [cm]	B_{field} [T]	Angle [deg]	Amp.turns [kA]	Cur. Dens. [A/cm^2]	Rigidity [Tm]
2.423	5.79	1.0	8.2	23.25	10500	17.2

The 2D Electromagnetic Design

The 2D electromagnetic design of the magnet provides a good measure for the determination of the geometry of the magnet, like the optimum dimensions of the iron's and coil's cross sections and the minimum thicknesses of the magnet's vacuum chamber and that of the pipe of the circulating beam which can withstand the magnetic and atmospheric forces. In the last subsection a method will also be presented to minimize the magnetic field within the vacuum pipe of the circulating beam region.

The cross section of the magnet The cross section of the magnet's iron has been chosen to keep the magnetic field in the iron below the value of 1.25 T when the magnet is excited at the field of 0.86 T. At such a field strength the magnet could deflect into the NSRL beam line charged particle with rigidity of 14.98 Tm. After few years of operation the D6 magnet was upgraded to extract ions with rigidity of 17.2 Tm at a field of 1.0 T. In this paper we will present results from the electromagnetic study of the magnet when it is excited at the field of 1 T. Fig. 4 shows a cross section of the current septum dipole magnet. The blue C-shape area is the iron of the magnet (yoke), the red colored rectangular areas are the conductors of the coil which consists of four conductors connected in series and the light-blue color ring is the vacuum pipe of the circulating beam. The green lines are the equipotential vector field lines

as calculated by the 2D OPERA computer code. Fig. 5 shows an expanded view of the cross section

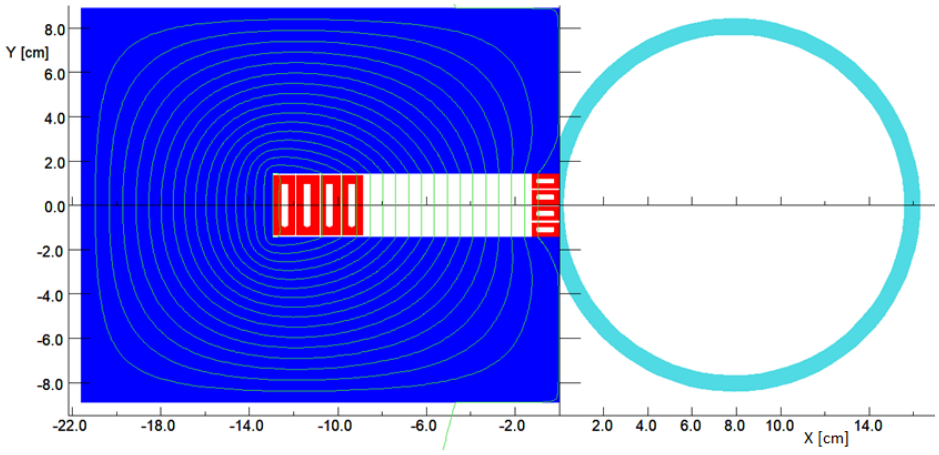

Figure 4: The cross section of the current septum dipole magnet. The blue C-shape area is the iron of the magnet, the red colored rectangular areas are the conductors of the coil which consists of four conductors connected in series. The cyan color ring is the vacuum pipe of the circulating beam. The green traces are the equipotential vector field lines as calculated by the 2D OPERA computer code.

at the septum region at the entrance of the magnet. The red hollow rectangles in Fig. 5 are the four conductors of the coil. The green area is part of the magnet's vacuum chamber made of nonmagnetic material, and the cyan colored region is part of the vacuum pipe of the circulating beam. The material of the vacuum pipe can be either magnetic or nonmagnetic however for reasons we explain below, the vacuum pipe of the D6 magnet is made of magnetic material. The dark blue areas on the top and bottom of the picture are part of the magnet's iron.

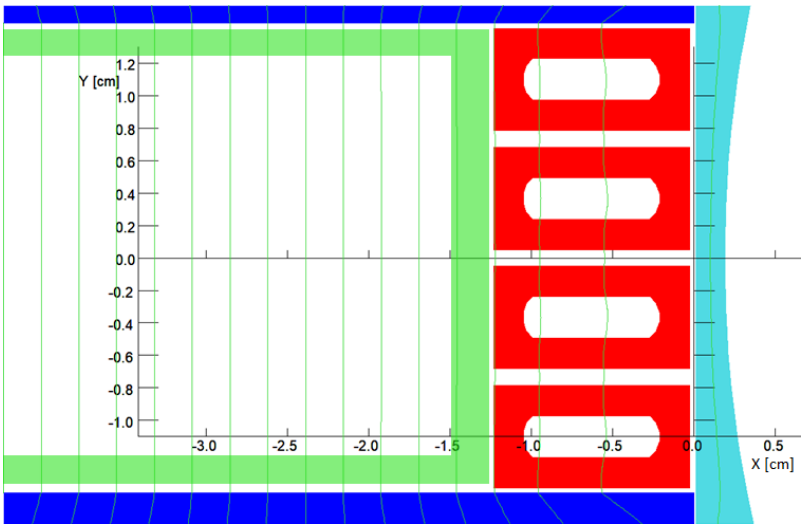

Figure 5: An expanded view of part of the cross-section of the magnet shown in Fig. 4 at the septum region. The red hollow rectangles are the four conductors of the magnet's coil, the green area is part of the magnet's vacuum chamber and the cyan colored region is the part of the vacuum pipe of the circulating beam. The dark blue areas on the top and bottom of the picture are part of the magnet's iron.

Magnetic field properties of the magnet As we mentioned earlier the magnet can be excited to a maximum magnetic field of $\simeq$1.0 T which allows the extraction from the AGS-Booster ions with rigidity of 17.2 Tm. Results on the magnetic field properties at the various regions of the magnet will be presented when the magnet is excited at this maximum field of $\simeq$1.0 T. The B_y component of the

magnetic field in the main field region of the magnet is shown in Fig. 6 . The black curve in Fig. 6 corresponds to the case when the pipe of the circulating beam is made of nonmagnetic material and the red curve is the B_y field for a pipe made of magnetic material which is the material of the D6 magnet's pipe. The B_y field which is described by the blue curve will be discussed latter on in this subsection. The right and left limits of the x-axis of the plot are the left and right inner surfaces of the magnet's vacuum chamber. The field uniformity of the magnet's main field region along the median plane is

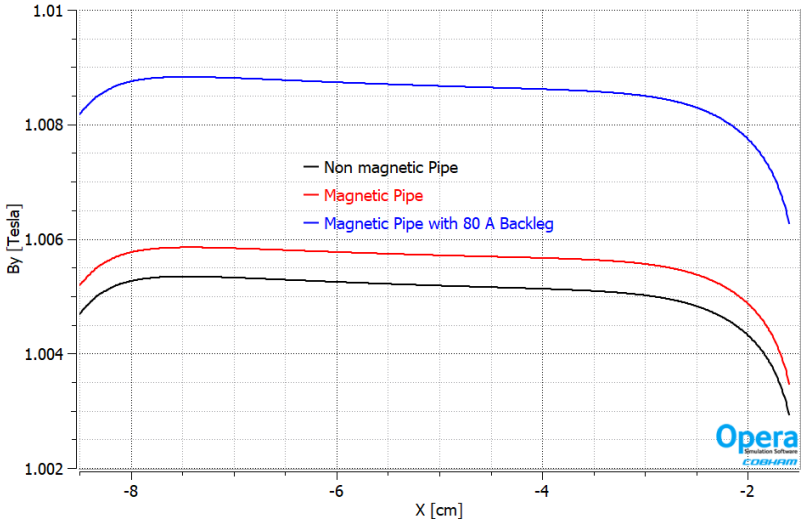

Figure 6: The B_y component of the magnetic field in the main field region of the magnet. The black curve corresponds to the case when the pipe of the circulating beam is made of nonmagnetic material and the red curve to that when the pipe is made of magnetic material. The nature of the blue curve will be discussed further down in this subsection.

plotted in Fig. 7 for the three cases corresponding to Fig. 6. The comparison of the black and red curves

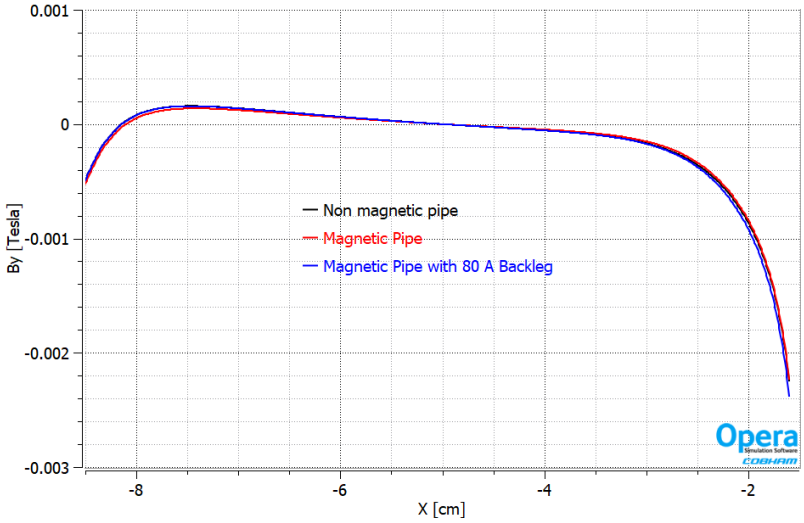

Figure 7: The magnetic field uniformity in the main field region of the magnet along the median plane for each of the cases corresponding to Fig. 6. The right and left limits of the x-axis of the plot are the left and right inner surfaces of the magnet's vacuum chamber. The field uniformity is not affected by the material of the pipe.

in Fig. 6 shows that the magnetic material of the pipe affects somewhat the strength of the magnetic field in the main field region but the required field can be achieved by adjusting the current of the power supply without affecting the field uniformity. Indeed the magnet's field uniformity for each of the three different cases of the magnetic field plotted in Fig. 6 is plotted in Fig. 7 and the plots in this figure show that the field uniformity is almost identical for all the three cases which are labeled on the plot. The

required current running in each of the four conductors of the coil to achieve the field of 1.0 T, is 5812 A and the maximum current density in each of the conductors of the septum region is 10500 A/cm^2. Such a high current density in the conductor has been achieved by improving the coil's water cooling system which is described in the APPENDIX I. The dimensions of the magnet's yoke have been chosen for the iron of the magnet to allow a maximum field of 1.25 T when the magnet was excited to 0.86 T. After the upgrade of the magnet's cooling system (see APPENDIX I) the magnet can be excited to the field of 1.0 T and Fig. 8 hows the contours of the magnetic field modulus (B_{mod}) over the magnet's iron yoke when the magnet is excited at the field of 1.0 T. Fig. 9 is the cross section of the magnet near

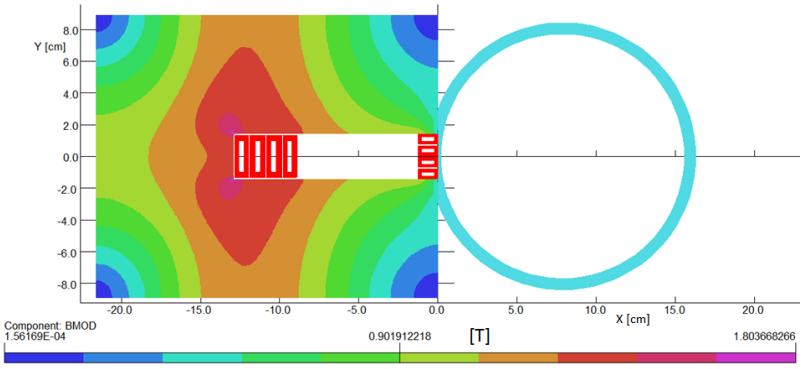

Figure 8: The contours of the B_{mod} of the magnet's yoke when the magnet is excited at its maximum field of 1.0 T. The yoke material is not saturated except at small regions near the two corners which are shared by the yoke and the magnet's gap.

the septum area, showing the location of the extracted beam (blue circle) and of the circulating beam (green circle) over the contours of the B_{mod}. The circulating beam is usually moved close to the septum by using a "local beam bump" which minimizes the strength of the extraction kicker. The contours of B_{mod} plotted in Fig. 9 over the circulating beam show a strength of 26 Gauss when the material of the vacuum pipe is nonmagnetic. It is of great importance that the strength of the magnetic field inside the vacuum pipe of the circulating beam is as low as possible to minimize its effect on the circulating beam.

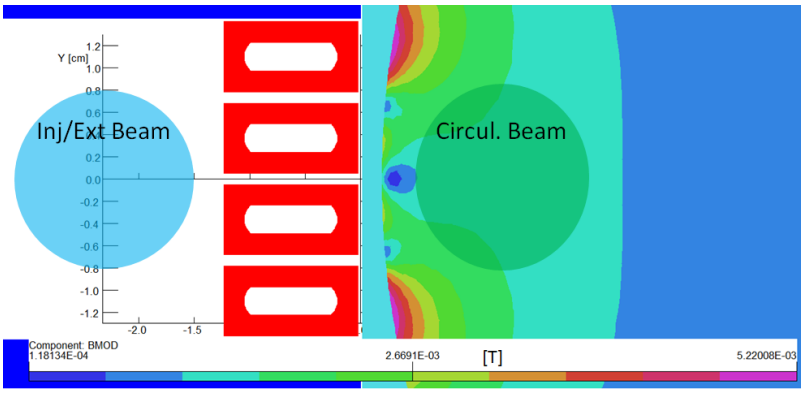

Figure 9: A cross section of the magnet near the septum region, showing the position of the extracted beam (blue circle) and of the circulating beam (green circle). The circulating beam is usually moved close to the septum by using a "local beam bump" which minimizes the strength of the extraction kicker. The colored contours is the strength of the B_{mod} which is $\simeq$26 Gauss at the place of the circulating beam (green circle). In this simulation the material of the vacuum pipe is nonmagnetic.

The back-leg winding In this subsection a method is described to minimize the magnetic field in the circulating beam region. Fig. 10 is the same a Fig. 9 but the circulating beam pipe is of "soft" magnetic material like steel 1006. The colored contours in Fig. 10 show that the strength of the B_{mod} at the region of the circulating beam region has been reduced significantly down to $\simeq$6 Gauss. Although the

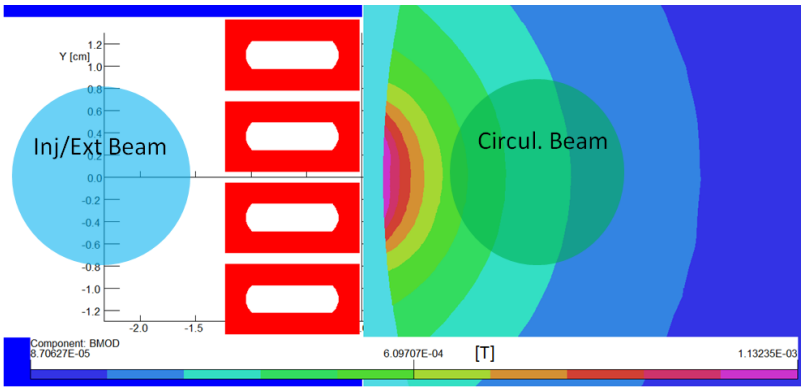

Figure 10: A cross section of the magnet near the septum area. This figure is similar to Fig. 9 except the material of the pipe for the circulating beam is of magnetic material. The colored contours is the strength of the B_{mod} with a maximum field of ≃6 Gauss at the place of the circulating beam (green circle).

strength of the magnetic field in the circulating beam region is reduced from 26 Gauss to 6 Gauss when the nonmagnetic vacuum pipe is replaced with a magnetic one, the magnetic field of 6 Gauss may still be large enough to affect the trajectory of an ion beam with low rigidity of ≃0.307 Tm. The near saturation of the material at the septum region is one of the reasons of a relatively large B-field in the circulating beam region when the vacuum tube is magnetic. This is a consequence of the the boundary condition which requires that the tangential magnetic field H|| to be continuous at the inner interface of the magnetic iron with the vacuum. The relations below elucidate the effect of the iron's saturation on the field inside the pipe.

$H||_{air}=H||_{iron} \Longrightarrow B||_{air}\ /\mu_0=B||_{iron}\ /(\mu_0\mu) \Longrightarrow B||_{air}=B||_{iron}\ /\mu.$

From the last relation we see that the B field in the circulating field region will be very small when the iron is not saturated ($\mu >> 1$). The colored contours on the area of the magnetic iron on the left picture of Fig. 11 show the strength of the magnetic field inside the iron tube and the colored contours on the right picture of Fig. 11 show the permeability. One way to further reduce the strength of the

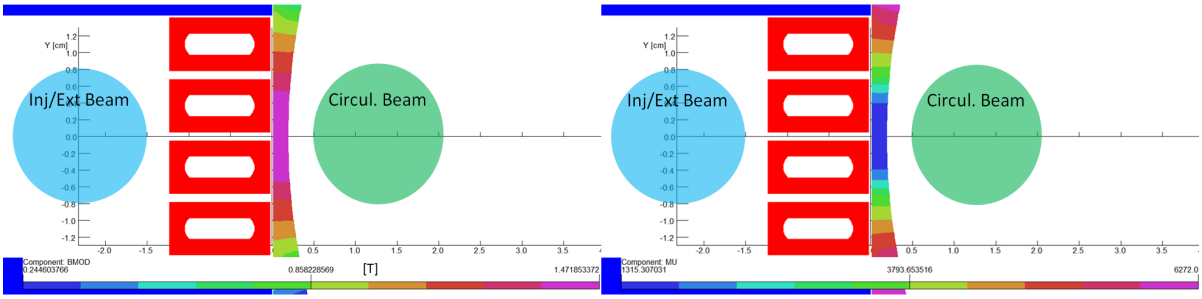

Figure 11: (Left) Colored contours of the B_{mod} inside the iron of the circulating beam pipe at the septum region. The iron is approaching saturation resulting in the reduction of the magnetic permeability's value. (Right) The value of the magnetic permeability of the iron at the septum is rather low ≃1300 as it is shown by the colored contours of the right picture and this makes the field inside the pipe rather large ≃6 Gauss.

magnetic field in the circulating beam region is to reduce the saturation of the iron in the septum region therefore increase the value of the magnetic permeability μ. This can be accomplished by placing a coil (back-leg winding) around the return yoke of the magnet. Such a coils is shown schematically by the small green rectangles in Fig. 12. Calculations show that when the back-leg winding carries a current of 88 A·turns, it reduces the magnetic field inside the vacuum beam pipe down to few mGauss as it is shown in Fig. 13 from the contour plot of the B_{mod} inside the circulating beam region. This field is to be compared with the corresponding field in Fig. 10 which has a strength of few Gauss. The effect of the current of the back-leg winding on the main field is an increase of 0.2%, as shown by the plot of B_y

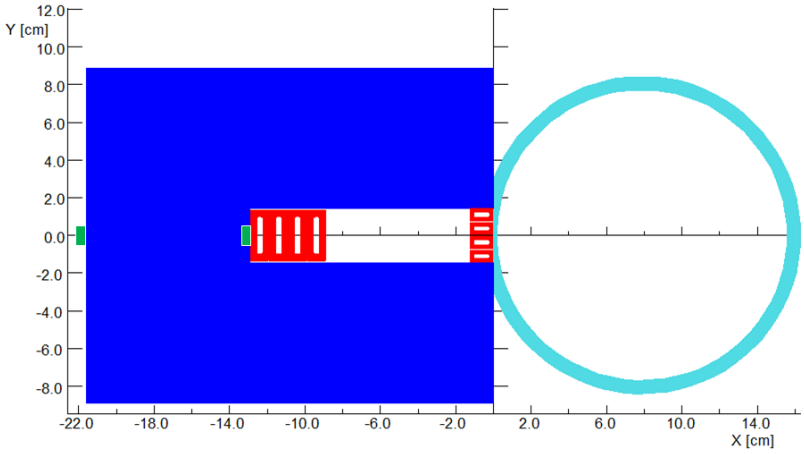

Figure 12: The cross section at the entrance of the septum magnet. The green rectangles represent a coil wound around the return yoke of the magnet (back-leg winding) to reduce the saturation of the vacuum pipe at the septum region. The back-leg winding is powered at a current of 88 Aturns.

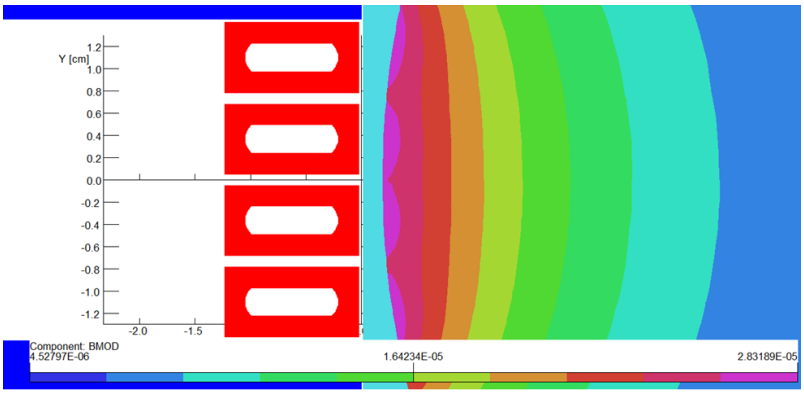

Figure 13: Contour plots of the magnetic field modulus in the circulating field region when the back-leg winding is powered by 88 Aturns. The strength of the field has been reduced to few mGauss. The effect of the back-leg winding on the field in the main field region can be compensated by the magnet's power supply with no effect the its field uniformity.

(blue curve) in Fig. 6. This increase in the main field of the magnet can be compensated by adjusting the current of the magnet's power supply with no change in the uniformity of the magnet's magnetic field. The current of the back-leg winding, generates inside the thin wall of the magnetic material of the pipe a field with an opposite direction to that generated by the main magnet. This field reduces the B-field in the thin septum pipe below saturation therefore it increases the value of the permeability μ of the magnetic material. Fig. 14 (Left) are the contours of the B_{mod} inside the pipe and the Fig. 14 (Right) shows the permeability inside the pipe when the back-leg winding is powered at 88 A·turns. Comparison of Fig. 14 with Fig. 11 shows that the effect of the back-leg winding reduces the B field inside the wall of the vacuum pipe from 1.47 Tesla to 0.04 Tesla and increases the permeability of the pipe from 1300 to 6300.

The 3D electromagnetic design

The 2D electromagnetic design of a magnet provides an accurate method to calculate the dimensions of the magnet's iron yoke to prevent the iron from saturation, calculate the coil size to keep the Ohmic losses at a reasonable level, and also to calculate the minimum thicknesses of the vacuum chambers which can withstand the electromagnetic forces and also prevent the collapse of the pipe under the atmospheric pressure. In addition the 2D design provides good guidance to modify the pole shape of the magnet to optimize its field uniformity. For a septum magnet the 2D design does not provide a

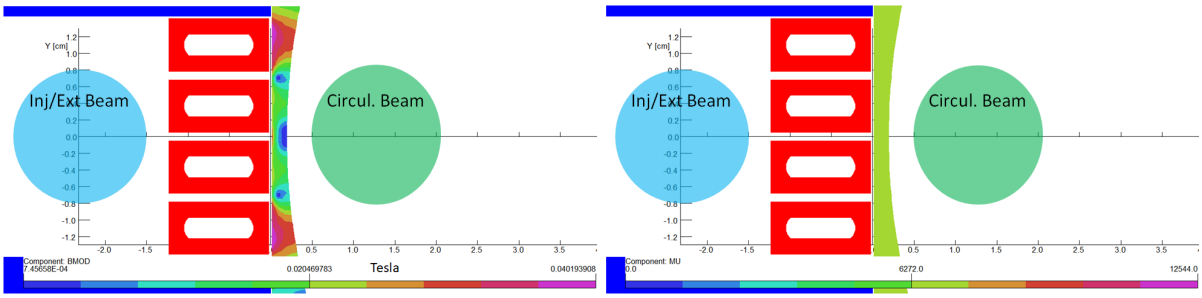

Figure 14: (Left) Colored contours of the B_{mod} inside the iron of the vacuum pipe, and (Right) colored contours of the permeability of the iron pipe when the back-leg winding is powered at 88 A·turns. Comparison of this figure with Fig. 11 shows that the effect of the back-leg winding reduces the B field inside the wall of the vacuum pipe from 1.47 Tesla to 0.04 Tesla and increases the permeability of the pipe from 1300 to 6300.

complete study of the magnet's field because the cross section of the magnet varies along the length of the magnet as shown by the isometric views of the magnet's two pictures at the bottom of Fig. 15 where the distance of the circulating beam pipe from the magnet increases. Therefore the 3D study is required to provide an accurate field not only inside the vacuum pipe of the circulating beam but also at the entrance and exit of the pipe. In addition the 3D design will provide information on the effect of the back-leg winding, mentioned earlier, on the magnetic field in the circulating beam region.

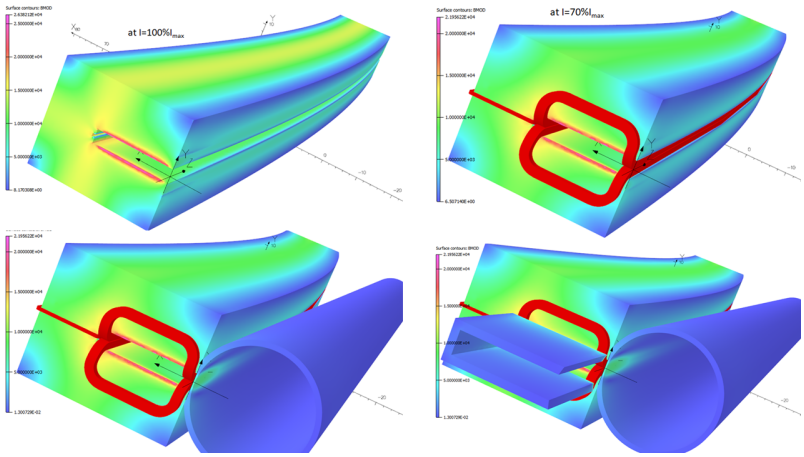

Figure 15: Isometric views of the septum magnet. (Upper left) Magnet iron only with contour plots of the B_{mod} on the surface of the iron. (Upper right) Magnet iron with coils with magnet excited at 70% of its maximum strength. (Lower left) Magnet iron, coils and pipe of circulating beam. (Lower right) Magnet iron, coils, pipe of circulating beam and field clamp.

The B-field in the circulating beam region

The 2D study of the magnet showed that the use of soft magnetic material for the pipe of the circulating beam reduces the magnetic field inside the pipe, with additional reduction of the field by the use of the back-leg winding. Results from the 3D study provide the B field not only inside the pipe region but also at the entrance and exit of the pipe. As an example the B_y component of the field plotted in Fig. 17 is along the orange line shown in Fig. 16. The orange line in Fig. 16 is along the z-direction on the median plane and at a distance 0.3 cm away from the inside surface of the pipe of the circulating beam. In Fig. 16 part of the circulating beam pipe at the entrance of the pipe has been removed to make the orange line more visible. The black trace in Fig. 17 is the plot of the B_y component (divided by a factor of 10) when the vacuum pipe is nonmagnetic. The red curve in Fig. 17 is the B_y component along this line when the pipe's material is magnetic, and a field clamp is placed at the entrance of the magnet. The beam pipe and the field clamp are magnetically connected to each

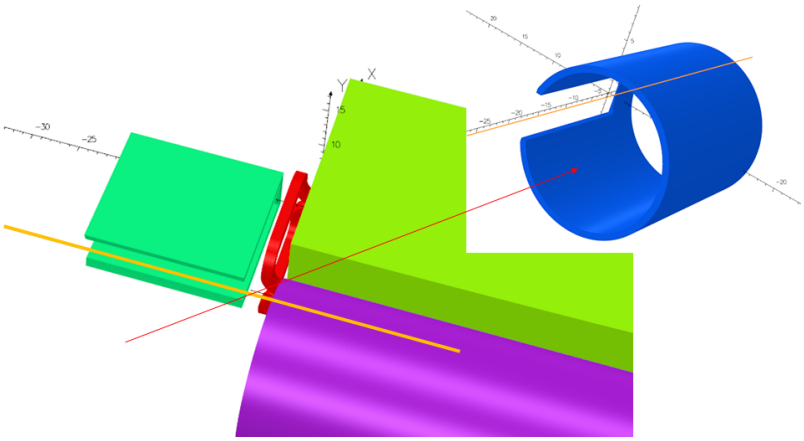

Figure 16: Along the thick orange line the plots of the B_y component of the field are shown in Fig. 17. The orange line is along the z direction and on the median plane at a distance 0.3 cm from the inner wall of the vacuum pipe. The front part of the pipe has been removed and placed on the top left corner of the figure to make the orange line visible.

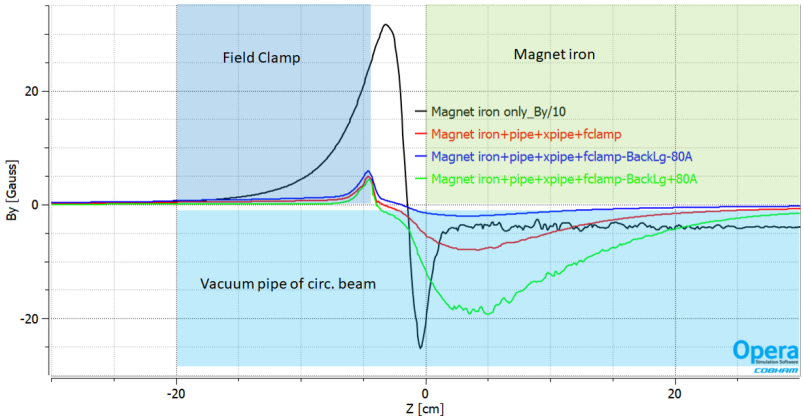

Figure 17: Plots of the B_y component of the field along the orange line which is shown in Fig. 16. The black trace is the plot of the B_y component when the vacuum pipe is nonmagnetic. Note the value of the B_y component of the field corresponding to the nonmagnetic pipe is divided by a factor of 10. The red curve is the B_y field corresponding to a magnetic beam pipe and field clamp. The blue and green traces correspond to the B_y components with the back-leg winding powered at -80 A and +80 A respectively.

other but not to the iron of the magnet. The blue and green traces correspond to the B_y components of the fields with the back-leg winding powered at -80 A and +80 A respectively. From the plots in Fig. 17 one concludes that the combination of the magnetic vacuum pipe with field clamp and a current of -80 A in the back-leg winding, reduces the magnetic field inside the pipe (blue trace in Fig. 17) to a very low value that will minimize the effect of this field on the low rigidity circulating beam. The highlighted regions on Fig. 17 is the top view of the magnet's iron, the beam pipe of the circulating beam, and the field clamp at the entrance of the magnet. Another way to realize the combined effect of the pipe's magnetic material and the -80 A current of the back-leg winding, on the trajectories of the low rigidity beam inside the beam pipe of the circulating beam is to compare the curves in Fig. 18. These curves shown in Fig. 18 are the trajectories of particles with rigidity 0.307 Tm circulating inside the pipe for three different cases as shown on the plot and explained in the figure caption. Among the three trajectories the one which corresponds to the case with iron pipe and back-leg winding -80 A (green trace) is the least affected by the field inside the pipe. Also Table 2 shows the position and direction of the low rigidity 0.307 Tm beam at the entrance and exit of the pipe for these three different cases. For this particular design of the D6 septum magnet the 3D calculations show that the effect of the back-leg winding is not as important as the 2D calculations show. The reason is that the distance of

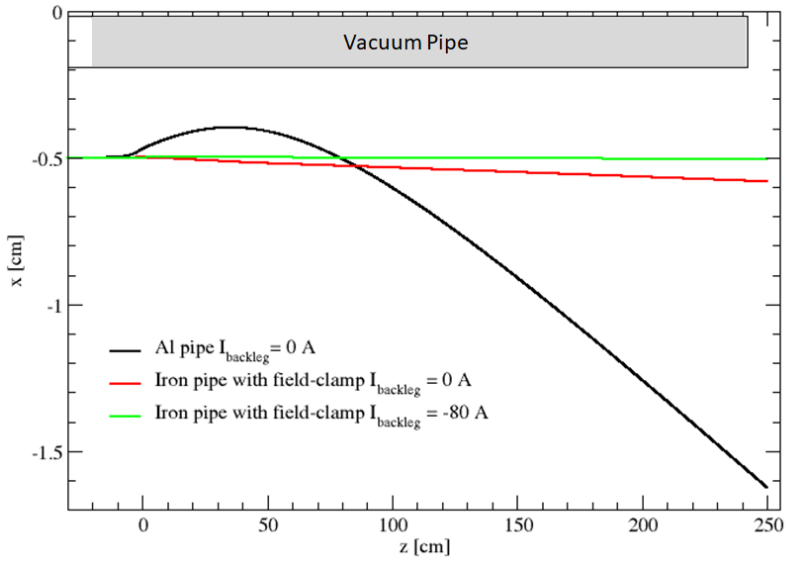

Figure 18: Three trajectories inside the pipe of the circulating beam for three different cases: a) Beam pipe made of nonmagnetic material (black trace). b) Beam pipe made of magnetic material (red trace). and c) Beam pipe of magnetic material and the back-leg winding with -80 A.

Table 2: The entrance and exit coordinates of a particle with rigidity 0.307 Tm traversing the vacuum pipe for three different cases mentioned in the figure caption of Fig. 18.

	Entrance			*Exit*		
	X_{in} [cm]	Z_{in} [cm]	X'_{in} [mrad]	X_{out} [cm]	Z_{out} cm]	X'_{out} [mrad]
Pipe nonmagnetic	-0.5	-30.0	0.0	-1.623	240.0	7.380
Pipe magnetic+field-clamp	-0.5	-30.0	0.0	-0.581	240.0	0.304
Pipe magnetic+field-clamp+Ibcl=80 [A]	-0.5	-30.0	0.0	-0.505	240.0	0.016

the vacuum pipe from the magnet is increasing rapidly as shown by the isometric views of the magnet in Fig. 15 and the thin wall of the magnetic pipe is not saturated as in the 2D case where the pipe is separated from the magnet's iron by only 0.152 mm. Fig. 19 is an isometric view the B_y component of the field (left) and the permeability μ (right) at the median plane over the area of the septum and at the entrance of the pipe. The maximum value of the magnetic field of 15 kG and the minimum value of the permeability μ 1000. Although these values indicate that the pipe is approaching saturation, this only happens in a small volume of the iron in the septum region, with the rest of the iron kept below saturation. Therefore the B field inside the pipe is not very high as we can see from the plot (red trace) in Fig. 17. In conclusion the 3D study shows that the effect of the back-leg winding is not as effective as in the 2D study because the pipe is close to saturation only in a small volume at the entrance of the magnet with the rest of the pipe being below saturation. Nevertheless by powering the back-leg winding to -80 A it is possible to minimize the B field in the circulating beam region as shown by the blue trace in Fig. 15 or by the green orbit in Fig. 18.

The B field in the main field region

Table 3 shows the integrated multipoles in the main field region when the septum magnet is excited at 1.0 T. The integrated multipoles have been calculated at a radius of 0.5 cm normal to the beam trajectory of a particle with the highest rigidity of 17.2 Tm that the magnet can bend by 8.2^o. The second row in Table 3 are the multipoles with back-leg winding powered at 0 A and the third row those with back-leg winding powered at -80 A. By comparing the multipoles in each of the two cases it is concluded that the back-leg winding does not affect the multipoles of the main field region. The slight

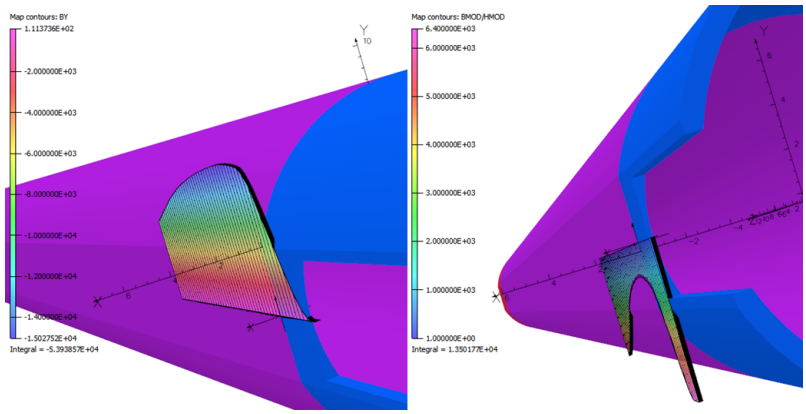

Figure 19: Isometric plots of the B_y component of the field (left) and the permeability (right) at the median plane over the septum area of the pipe at the entrance of the magnet. The maximum value (15 kG) of the B_y component of the magnetic field (left) and the minimum value (1000) of the permeability μ inside the magnetic material of the vacuum pipe both indicate that the pipe approaching saturation but only at small section of the pipe.

change of the integrated dipole multipole cause by the back-leg winding excited at a current of -88A can be compensated by adjusting the current of the magnet's power supply. The D6 septum magnet

Table 3: The integrated multipoles along the trajectory of a particle with rigidity 17.2 Tm at R=0.5 cm.

	Dipole [Gauss.cm]	Quad [Gauss.cm]	Sext [Gauss.cm]	Oct Gauss.cm	Dec [Gauss.cm]	12pole [Gauss.cm]
Back-leg = 0 [A]	2.492×10^6	239.2	7.98	0.59	1.72	0.73
Back-leg =80 [A]	2.502×10^6	256.2	-5.41	6.03	1.76	-0.07

is the first element of the NSRL beam line which generates uniform beam distributions at the target [1] . Prerequisite of the beam optics for uniform beams at the target location of the NSRL line is the Gaussian nature of the beam throughout the length of the beam line when the two octupoles [1] of the line are off. This suggests that all zero and first order elements of the beam line must contain very small values of multipoles (sextupoles, octupoles etc.) to not affect the Gaussian nature of the beam in the transport line. Calculations show that the strength of the higher order integrated multipoles which appear in Table 2 are too small to affect the measured beam uniformity at the NSRL target.

Experimental Results from Measurements on the D6 Septum Magnet of the NSRL Facility

Results from the experimental measurements on the D6 septum magnet of the NSRL test facility at BNL are shown in Fig. 20 which plots the experimental (black curve) and calculated (red curve) transfer functions of the septum magnet. The experimental measurements of the integrated dipole field were carried out with a 3 m long and 1.3 cm wide "flip-coil" which was bent by 8.2^o to follow the beam's trajectory. Since the built magnet and the model have the same geometry of the iron yoke, the small disagreement of the experimental and calculated transfer function is due to the different bh-curves of the iron used to manufacture the magnet and of the iron used in the calculations. The bh curve used in the calculations was the "default" bh-curve provided by the OPERA computer code [3].

CONCLUSIONS

A DC current septum magnet is being used successfully in the slow beam extraction region of the AGS-Booster to extract beams of various ion species for the NSRL facility at BNL [1,2] . The use of soft magnetic material for the circulating beam pipe is very important for the reduction of the B-field generated by the septum magnet in this region. A back-leg winding mounted on the septum's return

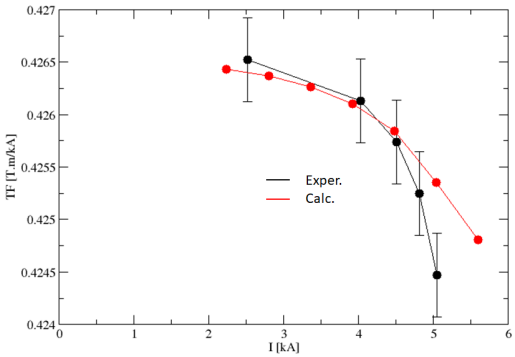

Figure 20: The transfer function of the septum magnet. The black curve corresponds to the results from the experimental measurements and the red curve from the 3D electromagnetic calculations. The small discrepancy is possibly due to the different bh curve of the iron used to manufacture the magnet and that used in the OPERA calculations.

yoke can provide additional reduction of the field in the circulating field region and can also be used to correct the orbit of the low rigidity beam circulating in the AGS-Booster.

ACKNOWLEDGEMENTS

The authors would like to thank the magnet division of the Collider Accelerator Department for the magnetic measurements of the D6 septum magnet.

APPENDIX I

To achieve such a high current density of 10500 A/cm^2 in the copper conductors, each of the four current conductors at the septum side of the magnet, was center tapped half way along the length of the magnet and the cooling water was fed to each conductor by four pipes from the top of the magnet. Fig. 21 are three isometric views of the four water pipes connected to the four conductors of the coil. Such an arrangement of the cooling system allows high current densities in the conductors because it reduces the pressure drop and the temperature gradient of the cooling water along the conductors. Fig. 22 is an actual picture of the brazing connection of one of the cooling pipes with one of the conductors.

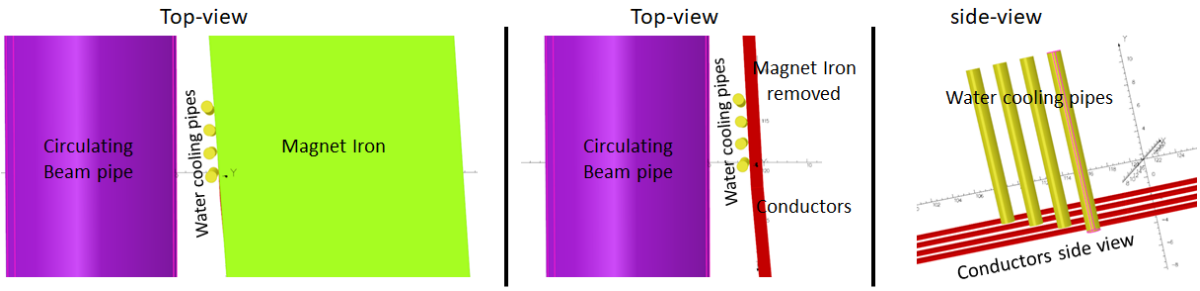

Figure 21: Isometric views of the four cooling water pipes each connected to the four conductors half way down the length of the magnet. Fig. 22 is an actual picture of the brazing connection of one of the cooling pipes with one of the conductors.

REFERENCES

[1] N. Tsoupas et. al. “Uniform beam distributions at the target of the NASA Space Radiation Laboratory’s beam line” Phys. Rev. ST Accel. Beams 10, 024701 2007

[2] K. Brown et. al. “The NASASpaceRadiationLaboratoryatBrookhavenNationalLaboratory: Preparation and delivery of ion beams for space radiation research” Nuclear Instruments and Methods in Physics Research A 618 (2010) 97–107

[3] Vector Fields Inc. http://www.vectorfields.com/.

Figure 22: A picture of the brazing connection of one of the cooling pipes with one of the four conductors of the coil.